Article

Nanometal Surface Energy Transfer in Optical Rulers, Breaking the FRET Barrier

C. S. Yun, A. Javier, T. Jennings, M. Fisher, S. Hira, S. Peterson, B. Hopkins, N. O. Reich, and G. F. Strouse

J. Am. Chem. Soc., **2005**, 127 (9), 3115-3119• DOI: 10.1021/ja043940i • Publication Date (Web): 11 February 2005

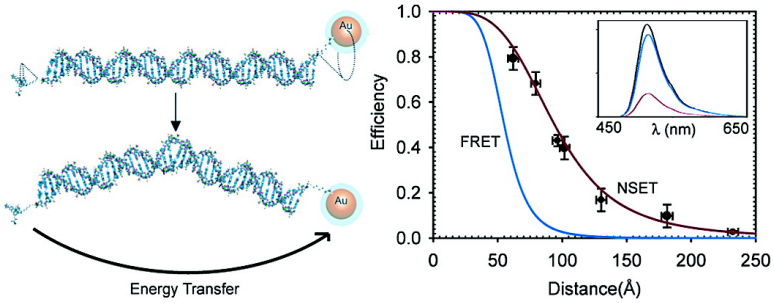

More About This Article

Additional resources and features associated with this article are available within the HTML version:

- Supporting Information
- Links to the 29 articles that cite this article, as of the time of this article download
- Access to high resolution figures
- Links to articles and content related to this article
- Copyright permission to reproduce figures and/or text from this article

View the Full Text HTML

J|A|C|S
ARTICLES
Published on Web 02/11/2005

Nanometal Surface Energy Transfer in Optical Rulers, Breaking the FRET Barrier

C. S. Yun,† A. Javier,† T. Jennings,† M. Fisher,† S. Hira,† S. Peterson,‡ B. Hopkins,‡ N. O. Reich,*,‡ and G. F. Strouse*,†

Contribution from the Department of Chemistry and Biochemistry, Florida State University, Tallahassee, Florida 32306-4390, and Department of Chemistry and Biochemistry and Program in Biomolecular Science and Engineering, University of California, Santa Barbara, California 93106-9510

Received October 5, 2004; E-mail: strouse@chem.fsu.edu

Abstract: Optical-based distance measurements are essential for tracking biomolecular conformational changes, drug discovery, and cell biology. Traditional Förster resonance energy transfer (FRET) is efficient for separation distances up to 100 Å. We report the first successful application of a dipole-surface type energy transfer from a molecular dipole to a nanometal surface that more than doubles the traditional Förster range (220 Å) and follows a $1/R^4$ distance dependence. We appended a 1.4 nm Au cluster to the 5′ end of one DNA strand as the energy acceptor and a fluorescein (FAM) to the 5′ end of the complementary strand as the energy donor. Analysis of the energy transfer on DNA lengths (15, 20, 30, 60bp), complemented by protein-induced DNA bending, provides the basis for fully mapping the extent of this dipole surface type mechanism over its entire usable range (50−250 Å). Further, protein function is fully compatible with these nanometal−DNA constructs. Significantly extending the range of optical based methods in molecular rulers is an important leap forward for biophysics.

Introduction

Recent interest in the study of larger, multicomponent complexes ranging from the ribosome to various nucleo-protein complexes require the ability to measure distance well-beyond the limits set by present optical methods. While significant progress in the study of such larger complexes has been made using X-ray crystallography, dynamic methods essential for a mechanistic understanding are limited. Dynamic changes are typically addressed by optical methods based on Förster resonance energy transfer (FRET) between molecular donors and acceptors, either organic[1,2] or metallic.[3,4] FRET technology is very convenient and can be applied routinely at the single molecule detection limit.[5] However, the length scale for detection in FRET-based methods is limited by the nature of the dipole−dipole mechanism, which effectively constrains the length scales to distances on the order of <100 Å($R_0 \approx 60$ Å).[6−8] Optical methods that do not alter the biomolecular function and which enable the investigation of both long range static and dynamic distances would facilitate studies of many multicomponent complexes that are presently difficult to measure. For example, nucleo-protein assemblies with broad biomedical significance often involve a constellation of proteins, which individually and in concert induce both large scale topological changes within the DNA, and regulate the expression of adjacent genes.

Since FRET physically originates from the weak electromagnetic coupling of two dipoles, one can imagine that the FRET limit can be circumvented by introducing additional dipoles and thus provides more coupling interactions. To fully grasp the consequences of this physical interaction, we must invoke the Fermi Golden Rule in the dipole approximation of energy transfer. The Golden Rule approximation relates the energy transfer rate (k_{EnT}) to a product of the interaction elements of the donor (F_D) and acceptor (F_A), $k_{EnT} \approx F_D F_A$. These interaction elements can be simplified such that their separation distance (d) dependencies are sole functions of their geometric arrangement. For single dipoles, $F \approx 1/d^3$, for a 2D dipole array, $F \approx 1/d$, and for a 3D dipole array, $F = constant$ such that the power of the distance factor decreases as the dimension increases.[9] FRET, which consists of two single dipoles, is easily derived from this rule such that $k_{FRET} \approx F_D F_A \approx (1/d^3)(1/d^3) \approx 1/d^6$. In fact, FRET is commonly written as $k_{FRET} = (1/\tau_D)(R_0/R)^6$. The Förster radius ($R_0$) is a function of the oscillator strengths of the donor and acceptor molecules, their mutual energetic resonance, and the vector addition of their dipoles. Typically this has a detectable distance limited to <100 Å.

Using a similar formalism, Chance, Prock, and Silbey[6] described the rate of energy transfer from a dipole to a metallic

† Florida State University.
‡ University of California.

(1) Lilly, D.; Wilson, T. *Curr. Opin. Chem. Biol.* **2000**, *4*, 507.
(2) Weiss, S. *Nat. Struct. Biol.* **2000**, *7*, 724.
(3) Dubertret, B.; Calame, M.; Libchaber, A. J. *Nat. Biotechnol.* **2001**, *19*, 365.
(4) Fritzsche, W.; Taton, T. *Nanotechnology* **2003**, *14*, R63.
(5) Neuweiler, H.; Sauer, M. *Curr. Pharm. Biotechnol.* **2004**, *5*, 285.
(6) Chance, R. R.; Prock, A.; Silbey, R. *Adv. Chem. Phys.* **1978**, *37*, 1.
(7) Förster, T. *Discuss. Faraday Soc. 27*, 1959.
(8) Lakowicz, J. R.; *Principles of fluorescence spectroscopy*, 2nd ed.; Kluwer Academic: Plenum: New York, 1999.
(9) Persson, B.; Lang, N. *Phys. Rev. B* **1982**, *26*, 5409.

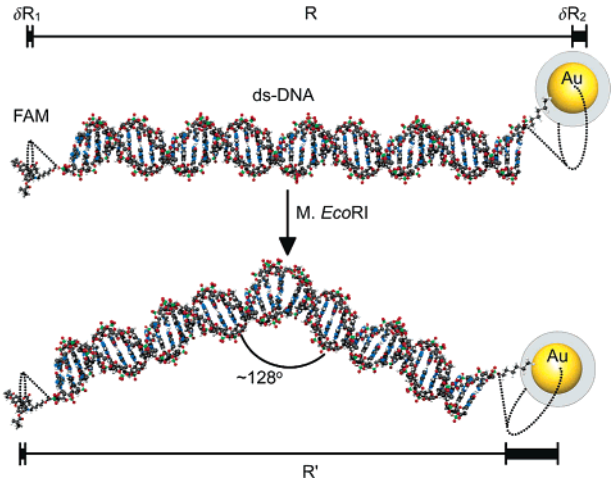

Figure 1. Schematic representation of the system we are studying, which consists of a fluorescein moiety (FAM) appended to ds-DNA of length R (varying from 15 to 60bp) with a Au nanoparticle ($d = 1.4$ nm) appended to the other end. The flexible C_6 linker produces a cone of uncertainty (δR) for both moieties. Addition of *M.EcoRI* bends the ds-DNA at the GAATTC site by 128°, producing a new effective distance R'.

surface[6,10,11] interband transition, which was further extended by Persson and Lang[9] to the metal's conduction electrons, in what can be called a surface energy transfer (SET) rate as $k_{SET} \approx F_D F_A \approx (1/d^3)(1/d) \approx 1/d^4$. Thus, energy transfer to a surface[9,10] follows a very different distance trend and magnitude of interaction. The exact form of dipole-surface energy transfer is $k_{SET} = (1/\tau_D)(d_0/d)^4$. The characteristic distance length is

$$d_0 = \left(0.525\frac{c^3\Phi_D}{\omega^2\omega_f k_f}\right)^{1/4} \quad (1)$$

and is a function of the donor quantum efficiency (Φ_D), the frequency of the donor electronic transition (ω), and the Fermi frequency (ω_f), and Fermi wavevector (k_f) of the metal.[6] The interaction of fluorophores with metal surfaces is different depending on the distance regime.[6] At very close distances (<10 Å), radiative rate enhancement is observed;[12] at intermediate distances (20−300 Å), energy transfer is the dominant process;[6,9] and at very large distances (>500 Å), fluorescence oscillations due to dipole-mirror effects take precedence.[6] In general, the quantum efficiency of energy transfer can be written as

$$\Phi_{EnT} = \frac{1}{1 + \left(\frac{r}{r_0}\right)^n} \quad (2)$$

In the case of dipole−dipole energy transfer, $n = 6$ and $r_0 = R_0$, while, for dipole-surface energy transfer, $n = 4$ and $r_0 = d_0$. This allows for the identification of the nature of the energy transfer mechanism from interrogation of the slope of a plot of energy transfer efficiency versus separation distance of the donor and acceptor. What will be the dominant quenching mechanism when a nanometer sized metal is used as the acceptor? Will the nanometal behave more like a dipole and be therefore FRET-like or will it behave more like a metal surface and be SET-like?

Methods

We can distinguish between FRET and SET processes by monitoring quenching efficiency by controlling the separation of a gold nanometal (Au(NM)) from a donor dye. This is achieved by appending fluorescein onto the 5′ end of DNA and a 1.4 nm diameter Au nanometal onto the opposing 5′ end of DNA using a six carbon spacer on the terminal phosphoramidite (Figure 1). The Au(NM) is a 1.4 nm single site monomaleimido-modified particle and was purchased from *Nanoprobes*. The DNA, purchased from *Midland Certified Reagent Co.*, is coupled to the Au(NM) through a 5′ C_6 alkanethiol functionality via a monomaleimido functional group. The donor dye is coupled in a similar fashion using a succinimidyl ester modified fluorescein (FAM). By varying the DNA lengths, the separation distance can be systematically varied between 62 Å and 232 Å (62 Å (15bp[a]), 96.4 Å (20bp[b]) 130.4 Å (30bp[c]), and 232.4 Å (60bp[d])).

[a]DNA Sequence: 5'FAM CGA CGA ATT CCG AGC; 5' HS GCT CGG AAT TCG TCG
[b]5' HS GCT GAT GCG AAT TCG AGG CG 5' FAM CG CCT CGA ATT CGC ATC AGC
[c]DNA Sequence: 5'FAM CGC CTA CTA CCG AAT TCG ATA GTC ATC AGC; 5' HS GCT GAT GAC TAT CGA ATT CGG TAG TAG GCG
[d]DNA Sequence: 5'FAM CAC TGA TGC TAT ACG GCT GAT GAC TAT CGA ATT CGG TAG TAG GCG AGC TCC TTC ATA GGC; 5' HS GCC TAT GAA GGA GCT CGC CTA CTA CCG AAT TCG ATA GTC ATC AGC CGT ATA GCA TCA GTG .

The persistence length of DNA is ~100bp and TEM analysis of Au(NM)−DNA−Au(NM) systems have shown that the assumption of persistence length distributions is valid. Buffered water was used to maintain a predictable DNA persistence length. In addition, water is also the most physiologically relevant medium for further applications.

All samples were deprotected and annealed according to literature procedures.[13,14] Continuous-wave photoluminescence measurements (cw-PL) and UV−visible absorption measurements were carried out on a Varian Eclipse fluorimeter and Varian Cary 50 Bio UV−vis spectrometer. The complexes were excited at the peak of the FAM absorption (472 nm).

To verify the change in photoluminescence intensity is a distance dependent phenomenon related to a SET process between the donor dye (FAM) and Au(NM), two control experiments were conducted using site-specific enzymes that recognize a GAATTC sequence located at the center of each DNA fragment. *EcoRI* endonuclease (*R. EcoRI*)was used to cleave the DNA, thereby allowing the dye and nanometal to diffuse apart, and *EcoRI* DNA methyltransferase (*M. EcoRI*) was used to induce a bend angle of 128° at the GAATTC site[15] (Figure 1). All experiments were carried out in buffer at rt by standard protocols with the exception that thiol based reductants were excluded to minimize the chance of Au(NM) degradation under the reaction conditions.

Results

A plot of the energy transfer efficiency versus separation distance of FAM-Au(NM) illustrates the distance-dependent behavior for energy transfer from a molecular dipole to a nanometal (Figure 2). The efficiency of energy transfer (E), where $E = 1 - I_d/I_\infty$, is monitored by cw-PL spectroscopy of the FAM moiety. The calculated distance assumes a linear DNA strand[16,17] with a C_6 spacer between the DNA and the donor dye moiety, as well as between the DNA and the Au(NM). The

(10) Alivisatos, A. P.; Waldeck, D. H.; Harris, C. B. *J. Chem. Phys.* **1985**, *82*, 541.
(11) Kuhnke, K.; Becker, R.; Epple, M.; Kern, K. *Phys. Rev. Lett.* **1997**, *79*, 3246.
(12) Dulkeith, E.; Morteani, A.; Niedereichholz, T.; Klar, T.; Feldmann, J.; Levi, S.; van Veggel, F.; Reinhoudt, D.; Möller, M.; Gittins, D. *Phys. Rev. Lett.* **2002**, *89*, 203002.
(13) Yun, C.; Khitrov, G.; Vegona, D.; Reich, N.; Strouse, G. *J. Am. Chem. Soc.* **2002**, *124*, 7644.
(14) Alivisatos, A.; Johnsson, K.; Peng, X.; Wilson, T.; Loweth, C.; Bruchez, M.; Schultz, P. *Nature (London)* **2002**, *382*, 609.
(15) Garcia, R.; Bustamante, C.; Reich, N. *Proc. Natl. Acad. Sci. U.S.A.* **1996**, *93*, 7618.
(16) Shellman, J. A. *Biopolymers* **1974**, *13*, 217.
(17) Frontali, C.; Dore, E.; Ferranto, A.; Gratton, E.; Bettini, A.; Pozzan, M. R.; Valdevit, E. *Biopolymers* **1979**, *18*, 1353.

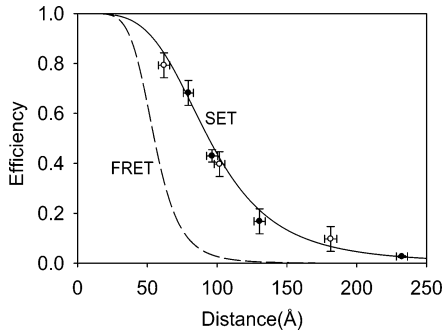

Figure 2. Energy transfer efficiency plotted versus separation distance between FAM and Au(NM). Filled circles (●) represent DNA lengths of 15bp, 20bp, 30bp, and 60bp. The measured efficiencies of these strands with the addition of *M.EcoRI* are represented by the open circles (○). The error bars reflect the standard error in repeated measurements of the fluorescence as well as the systematic error related to the flexibility of the C_6 linker as illustrated in Figure 1. The dashed line is the theoretical FRET efficiency, while the solid line is the theoretical SET efficiency.

error bars along the distance axis in Figure 2 represent the minimum and maximum approach for two conical positions of the FAM dye relative to the Au(NM)(Figure 1).

The 15bp fragment (62 Å) exhibits a 68.2% quenching of the emission of FAM relative to a FAM−DNA conjugate at equivalent concentration. The 20bp (96 Å), 30bp (130 Å), and 60bp (232 Å) exhibit quenching efficiencies of 44.0%, 16.7%, and 2.6% respectively (Figure 2). A plot of the actual PL data for the FAM appended DNA coupled to the Au(NM) and in the absence of Au(NM) is shown in Figure 1 in the Supporting Information. Upon addition of *M.EcoRI*, which induces a 128° bend at the center of these DNA constructs, the efficiency of energy transfer is increased to 79% for the 15 bp, 40% for the 30 bp, and 10% for the 60 bp. The enhanced quenching is expected since the change in the duplex structure from a linear to a bent structure closes the distance between the 5′ ends of each strand, thus bringing the FAM and Au(NM) quencher into closer proximity. This provides an opportunistic internal standard to test the validity of the nanometal surface energy transfer (NSET) for the donor dye to a nanometal surface. To ensure no interference in biological activity, the efficiency was monitored at various concentrations of *M.EcoRI*, and was found to fit the empirically accepted mass-action law for K_d.[18] Treatment with *R.EcoRI*, which cuts at the center of the DNA sequence, resulted in the FAM photoluminescence intensity at nearly the level of FAM in the absence of Au(NM) for all DNA constructs. This is consistent with quenching strictly arising from an energy transfer process in the conjugate structure (Supporting Information Figure 1). This is analogous to a molecular beacon experiment, in which the turn on of the fluorescence intensity following cutting is characteristic of the loss of energy transfer between the dye pairs.[19,20]

Discussion

Comparison of the experimental energy transfer efficiency values with the theoretical energy transfer efficiency curves for a pure dipole−dipole (FRET) and dipole-surface (SET) energy transfer process is shown in Figure 2. The Förster radius (R_0), calculated using Förster's equation,[7] is 59 Å, while the SET radius (d_0), calculated using Persson and Lang's equation,[9] is 94.3 Å. The d_0 value was calculated using $\Phi_D = 0.8$, $\omega = 3.8 \times 10^{15}$ s^{-1}, $\omega_f = 8.4 \times 10^{15}$ s^{-1}, and $k_f = 1.2 \times 10^8$ cm^{-1} which are bulk Au and FAM constants, while R_0 is calculated using the spectral overlap integral calculated from Au(NM) absorbance and FAM PL spectra.

Comparison of the quenching efficiency and slope indicates poor agreement with a Förster mechanism ($1/R^6$) and precise agreement with the ($1/R^4$) plot predicted for a dipole interacting with a metallic surface (SET). To assess the trend in distance independently from the theoretical predictions, the data were fit to eq 2 using r_0 and n as fitting parameters. For the six replicated experiments, the average values of n were 4.0 with an average r_0 of 92 Å, representing 50% quenching efficiency. This is in excellent agreement (< 2% error) with the theoretically calculated values for a SET mechanism ($d_0 = 94.3$ Å), while the strong discrepancy between the fit and the FRET model in terms of slope and distance eliminates FRET as the quenching mechanism.

SET does not require a resonant electronic transition, which is fundamental to a Förster process. The physical origin for SET is attributed to the interaction of the electromagnetic field of the donor dipole interacting with the nearly free conduction electrons of the accepting metal. These conduction electrons behave like a Fermi gas and will interact most strongly with the oscillating dipole if they travel near and perpendicular to the metal surface.[9] The dipole does not interact with a discrete resonant electronic transition, but rather an interaction with the electronic continuum levels of a metallic system. This is a surprising result, since this suggests a Au(NM) cluster similar in size to the FAM moiety can exhibit characteristically metal-like behavior and the Au(NM) acts like a metal surface with respect to the FAM dipole.

The plausibility of the proposed mechanism relies on an accurate interpretation of the electronic structure of the Au(NM). To achieve this, we have performed a semiempirical simulation of a Au(NM) with radius $r = 0.7$ nm. Using the Mie equation for very small metal particles,[21] we calculate the absorption coefficient(α) as a function of size and frequency,

$$\alpha(\omega,r) = \frac{K\eta^3\omega\epsilon_2(\omega,r)}{(\epsilon_1(\omega) + 2\eta^2)^2 + \epsilon_2(\omega,r)^2} \qquad (3)$$

where $K = 7.16 \times 10^{16} Q(s)$ and Q is the volume fraction of particles, ϵ_1 is the real part of the dielectric constant, ϵ_2 is the complex part of the dielectric constant ($\epsilon = \epsilon_1 + i\epsilon_2$), and η is the refractive index of the medium (in this case water, $\eta = 1.33$). Empirically obtained bulk Au values for ϵ_1 were used directly,[22,23] but for ϵ_2, a combination of empirically obtained ϵ_2 values[22,23] for bulk Au representing primarily interband transitions were combined with Drude-model[24] size-dependent calculations.[25,26] We used the following model[25] for the Drude calculations of a free electron gas using

(18) Mashhoon, N.; Reich, N. *Biochemistry* **1991**, *30*, 2933.
(19) Broude, N. E. *Trends Biotechnol.* **2002**, *20*, 249.
(20) Fang, X.; Li, J.; Perlette, J.; Tan, W.; Wang, K. *Anal. Chem.* **2000**, *72*, 747A.
(21) Kriebig, U.; Genzel, L. *Surf. Sci.* **1995**, *156*, 678.
(22) Otter, M. *Z. Physik* **1961**, *161*, 163.
(23) Theye, M. *Phys. Rev. B* **1970**, *2*, 3060.
(24) Ibach, H.; Lüth, H. *Solid-State Physics: An Introduction to Principles for Materials Science*, 2nd ed.; Springer: New York, 1995.
(25) Doremus, R. H.; Rao, P. *J. Mater. Res.* **1996**, *11*, 2834.
(26) Link, S.; El-Sayed, M. A. *J. Phys. Chem. B* **1999**, *103*, 4212.

$$\epsilon_2(\omega,r) = B + A\left(\frac{l_e}{r} + 1\right)\left(\frac{1}{\omega^3}\right) \quad (4)$$

with fitted empirical values[23] ($A = 4.74 \times 10^{-46}$ s^{-3}, $B = 0.10$), where l_e is the mean free electronic path in a Au crystalline film. Since the Drude model of ϵ_2 is intrinsically size-dependent, it crosses the size-independent bulk Au interband transition at different energies for each given size. These crossing points were used to determine over what ranges the system was strongly Drude-like. At small sizes, the Drude behavior dominates the entire visible and near-IR spectrum and a strong ω^4 trend is observed corresponding to free-electron absorption. At frequencies higher than the crossing point, interband absorption dominates and there is no size dependence in the absorption. At larger sizes, the free electron absorption develops coherent character and partly transforms into the surface plasmon resonance absorption band. The absorption spectrum simulated in this way appears in Figure 3 as the bottom graph.

As can be seen, the Drude-interband crossing point appears as a feature in the curve at 3.6 eV. At energies less than this, for example, the FAM dye used in this study ($E \approx 2.5$ eV), free electron behavior strongly dominates over interband transitions. The position of the drude-interband crossing point demonstrates that, at very small sizes, over the wavelength range of the emission of the fluorophore, the electronic properties are dominated by free electron gas behavior. While both dipole−dipole and dipole-metal surface energy transfer theories account for resonant interstate electronic transitions, only a variation of the dipole-surface version accounts for energy transfer to free conduction electrons. To verify the validity of our semiempirical simulation, the absorption spectrum of the ligand (Figure 3, middle graph) is added, allowing a complete fit of the experimental absorption spectrum of the Au(NM) complex-(Figure 3, top graph, dashed line). This fit (Figure 3, top graph, solid line) is in good agreement with the experimental absorption spectrum. The deviation at higher energies is most likely a result of a shift in the electronic structure of the ligand due to binding to the nanometal surface. In addition, at 2.4 eV, while our semiempirical simulation predicts the presence of the surface plasmon resonance band, it is slightly more pronounced in the actual experimental spectrum. At this size regime, a Au(NM)'s electrons are best described as having noncoherent character with only minor evidence of coherent behavior but clearly have negligible interband transitions, specifically over the energies of interest.

It is clear that the Au(NM) is not an infinitely wide plane of dipoles and that the true n should be slightly greater than 4. However, the data set does suggest that, within experimental error, there is a virtual plane of dipoles on the nanometal that the donor dipole interacts with and that while there are undoubtedly other interactions that are present, this appears to be the dominant interaction. In addition, due to the large surface-to-volume ratio of small clusters and sizes much smaller than the mean free electronic path[24](~410 Å in Au), the conduction electrons are very likely to be found near the surface such that these small clusters are more accurately described as fragments of metal surfaces, rather than fragments of bulk metal crystals. This strong surfacelike character is what is most likely responsible for the observed distance dependence. The excellent agreement between the theoretical and experimental plots

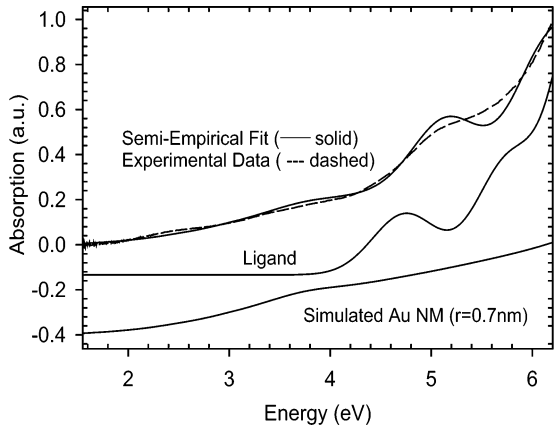

Figure 3. Comparison of the experimentally obtained absorption spectrum of Au(NM) (top graph, dashed line) with a semiempirical fit (top graph, solid line) using the experimentally obtained ligand spectrum (middle graph) and the semiempirical simulation of Au(NM) (bottom graph)

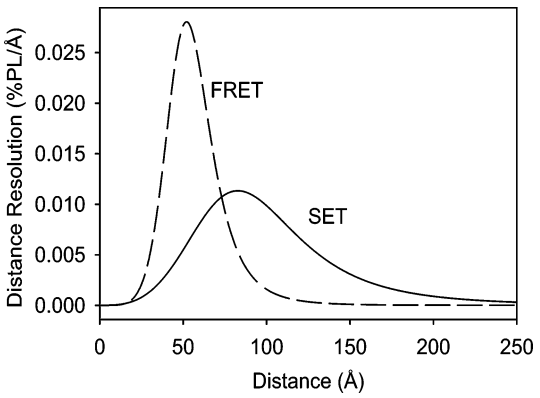

Figure 4. Separation distance-dependent length resolution of the FRET and SET mechanisms. This plots the distance derivatives of the SET (solid line) and FRET (dashed line) curves of Figure 2. The crossing of the two curves indicates the distance at which the 2 methods have identical resolution.

implies that if a size correction to SET exists, it must be a very small correction for this particular system.

To compare the strengths and weaknesses of FRET and SET, it is beneficial to inspect the first derivative with respect to separation distance ($\partial/\partial r$) in Figure 4, which represents the overall length resolution of each method as a function of separation distance. The FRET peak is tall, which implies that FRET is a highly sensitive method. However, it is also very narrow, which suggests the range of detection is also very limited and centered about the range of R_0. In addition, the FRET peak does not extend past 100 Å. The SET curve follows a different trend, being broader and shorter than the FRET curve. Although SET does not have the sensitivity of FRET, it more than makes up for this limitation in both its total usable distance range and its maximum limit of detection. Where FRET resolution essentially drops to insignificance at 100 Å, SET continues to provide similar distance resolution even up to 220 Å. As can be seen from Figure 4, below ~70 Å (the point where the SET and FRET curves intersect is the distance at which they have identical resolution), FRET provides the best distance resolution. However, above ~70 Å, SET provides better resolution than FRET, and this is clearly the better of the two methods at extremely long distances. Intuitively we can imagine FRET as a very short ruler with finely spaced markings, while SET is a very long ruler (more than twice the length of FRET)

with widely spaced markings (nearly double the spacing of FRET). Although both SET and FRET rely on dipolar coupling, we intuitively expect SET to have a longer distance dependence due to the cooperative effect of more accessible acceptor dipoles yielding more dipolar interactions. The advantage that our DNA system affords is that these two effects can be directly compared simply by changing the acceptor molecule.

Conclusion

The power of optical based molecular rulers is the ability to measure subtle changes in structure following an event, particularly in biological systems. For instance, measuring distances in excess of 150 Å is desirable for diverse applications including nucleo-protein assemblies involving DNA duplexes where large-scale conformational changes are seen. The NSET approach described here provides a basis for achieving the distances to deconvolute such a complex and important interactions. The observation of energy transfer between a dipole and a metal nanosurface provides a new paradigm for design of optical based molecular ruler strategies at distances more than double the distances achievable using traditional dipole−dipole Coulombic energy transfer based FRET methods.

Acknowledgment. This work was supported by the National Institute of Health (5R01EB000832). G.F.S. and T.J. thank MARTECH-FSU.

Supporting Information Available: Fluorescence spectra of DNA−Au(NM) constructs. This material is available free of charge via the Internet at http://pubs.acs.org.

JA043940I